Dual-Band Bandpass Filter Optimized for High Q-Factor

Walid M. Fahmy [1], Asmaa E. Farahat [1], Khalid F. A. Hussein [1], and Abd-El-Hadi A. Ammar [2]

[1] Microwave Engineering Department
Electronics Research Institute, Cairo, Egypt
walidfahmy48@yahoo.com, asmaa@eri.sci.eg, khalid_elgabaly@yahoo.com

[2] Electronics and Electrical Communications Department, Faculty of Engineering, El-Azhar University, Cairo, Egypt
hady42amar@gmail.com

Abstract ─ High quality factor bandpass filters based on a number of cascaded resonators of dual-resonance mechanism are proposed in the present paper. Each resonator is constructed as two overlapped coplanar waveguide (CPW) resonant structures. The cascaded resonators mediate microwave coupling between two isolated corner-shaped CPW feeders only at the resonant frequencies leading to a bandpass filter of high quality factor. The two resonant frequencies and the separation between them can be fine-tuned by the dimensions of the structure. The effects of the dimensional parameters of the resonator and the feeding CPW regions on the resonant frequencies and the performance of the bandpass filter are investigated. The effect of the loss tangent of the dielectric substrate material on the quality factors at the two resonant frequencies is studied. Three prototypes of the proposed filter are fabricated and experimentally studied for more understanding of the underlying physical principles of operation and for verifying some of the simulation results. The experimental results show good agreement when compared with the corresponding simulation results. It is shown that, at low enough absolute temperature, the proposed structure can operate as superconducting microwave resonator when made from the appropriate materials. Also, it is shown that an optimized design of the proposed bandpass filter, based on superconducting CPWR structure, can achieve quality factors high enough to form a quantum data bus for hybrid architecture of quantum information systems.

Index Terms ─ Band-pass filter, dual-band filter, high-Q filter.

I. INTRODUCTION

A coplanar waveguide (CPW) has the principal advantage that the signal line and the signal grounds are placed on the same substrate surface. This eliminates the need for via holes and, thereby, simplifies the circuit fabrication. Moreover, this allows simple connection of series as well as shunt components [1]. Another main advantage of the CPW is that it exhibits lower conductor loss than microstrip lines [2], [3]. CPW parameters are not sensitive to the substrate thickness, and a wide range of impedance is achievable on reasonably thick substrates. Also, circuits can be built using both the odd and the even CPW modes [4]. Moreover, CPWs are open structures, and do not require metallic enclosures [4].

CPW resonators have their distributed element construction avoiding uncontrolled stray inductances and capacitances, and, thereby, have better microwave properties than lumped element resonators [5]. Another advantage of CPW structures practically arises when performing microwave measurements; that is a series of CPW resonators with different frequencies can be measured using a single feed line, which greatly simplifies the measurement process [6].

The end-coupled and edge-coupled CPW resonator structures are commonly used for microwave and millimeter-wave filter design [7]. In end-coupled resonators, the interchange of energy with the coupling gap may be insufficient, even when very narrow gaps are employed. Due to this reason parallel- or edge-coupled CPWRs are more commonly used than end-coupled CPWRs [7]. Planar structures based on the edge-coupled CPW have been developed as circuit elements for monolithic microwave integrated circuits (MMIC's) [8].

Due to their practical importance, microwave and millimeter-wave bandpass filter design based on CPWRs has attracted the attention of many research works. In [1], the design of high-quality bandpass filter employing shunt inductively coupled CPW resonators is introduced and shown to exhibit low radiation loss due to the removal of the capacitively coupled gaps encountered in bandpass filter employing end or edge coupled CPW resonators. In [9], a cross-coupled CPW structure design is proposed for bandpass filter, which is constructed by cascading several sections of quarter wavelength open-end series stubs. In [10] and [11], compact edge-coupled

Submitted On: December 17, 2019
Accepted On: January 28, 2021

https://doi.org/10.47037/2020.ACES.J.360405

CPW bandpass filter designs are proposed for operation at microwave and millimeter-wave frequencies.

Superconducting CPWRs with large internal quality factors of typically several hundred thousand can be routinely realized [5]. Such resonators find a wide range of applications as radiation detectors in the optical, ultraviolet, and x-ray frequency range, in parametric amplifiers, for magnetic field tunable resonators and to act as quantum data bus for superconducting qubits [6], [5].

The present work proposes a design of a bandpass filter of high quality factor. The proposed filter is constructed as two feeding CPW regions which are parallel-coupled (or edge-coupled) to a CPW resonating structure. As long as the operating frequency is far from the resonant frequencies of the CPW resonating structure, the feeding CPW regions are isolated from each other preventing any possible power transfer from one port of the filter to the other. Only at the resonant frequencies the feeding CPW regions are coupled to each other via the CPW resonating structure and, thereby, allowing power transfer between the filter ports. Some prototypes of the proposed filter are fabricated and experimentally studied for more understanding of the underlying physical principles of operation and for verifying some of the simulation results. The experimental results show good agreement when compared with the corresponding simulation results. Near zero-Kelvin absolute temperature, the proposed structure can operate as superconducting microwave resonator when made from the appropriate materials, where a quality factor high enough to form a quantum data bus for hybrid architecture of quantum information systems can be achieved.

II. PROPOSED BANDPASS FILTER DESIGNS

The proposed bandpass filter has the sketch of its geometry shown in Fig. 1 with the indicated symbolic dimensional parameters. This filter is constructed as two feeding (normally isolated) corner-shaped CPW regions which are (capacitively) parallel-coupled (at resonance) to the dual-resonant CPW structure. The design of higher-order BPF for each pass-band can be based on using cascaded resonators to mediate coupling between the isolated CPW feeding regions as shown in Fig. 1 (a).

For the design shown in Fig. 2, the dual-resonator structure can be considered as composed of two overlapped resonators. One of them is a half-wavelength CPWR, which is short-circuited at its both ends and forms the perimeter of U-shape. The other resonator is a straight CPWR of relatively wide central conductor formed by the area subtended between the arms of the U-shape. This CPWR is open-circuited at the base of the U-shape and short-circuited at the other end (top of the U-shape) and, thus forms a quarter-wavelength resonator. As long as the operating frequency is far from the resonant frequencies of the dual CPWR structure, the corner-shaped CPW feeding regions are isolated from each other leading to zero power transfer between the filter ports (1) and (2). Only at the resonant frequencies, the CPW feeders are parallel-coupled to the dual-resonant CPW structure and, hence, the power transfer can occur only at these frequencies leading to high-quality factor bandpass filter response.

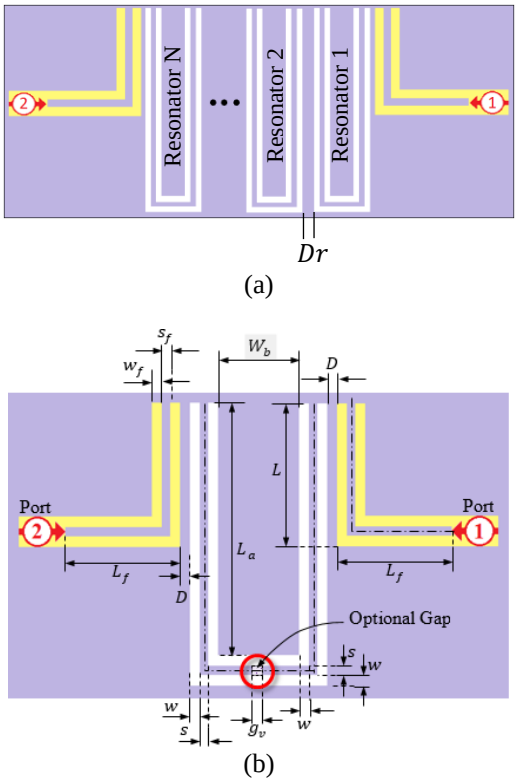

Fig. 1. Schematic of the proposed design for high quality-factor dual-band BPF: (a) Higher-order BPF based on cascaded CPW resonators, and (b) dimensional parameters.

A dual-bandpass filter design is shown in Fig. 3, which can be considered as a modification of the filter design shown in Fig. 2. The difference is a gap made in the central conductor of the short-ended CPW region forming the perimeter of the U-shape. The gap divides the U-shaped CPW region into two symmetric CPW regions of mirrored-L shape; each of them is short-circuited at one end and open-circuited at the other end and, thus, forming two identical quarter-wavelength resonators.

A single-bandpass filter design is shown in Fig. 4. This design can be considered as a modification of the design shown in Fig. 3 by making two other gaps; each gap is cut in one of the central conductors of the two quarter-wavelength resonators forming the mirrored-L shape. The purpose of these gaps is to diminish or damp

the resonance of the two quarter-wavelength CPW resonators forming the mirrored-L so as to get the new design working as a high-quality-factor single-bandpass filter.

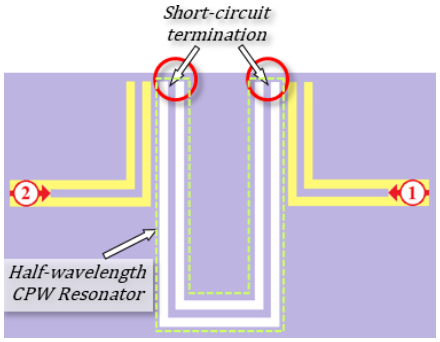

(a) The first resonant mechanism (Lower pass band)

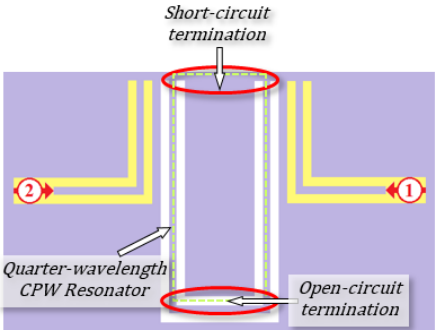

(b) The second resonant mechanism (Upper pass band)

Fig. 2. Mechanisms of resonance in the proposed bandpass filter based on dual-CPWR structure.

III. THEORETICAL BASIS OF OPERATION

For simplified analysis of the proposed bandpass filter designs, simple configurations of end-coupled CPWRs are considered. The simplest method to create a CPWR is to make a gap in the central conductor as shown in Fig. 5 (a) or to short the central conductor to the side (ground) conductors as shown in Fig. 5 (b). The gap can be considered as a series capacitance C_g between the central conductor of the feeder waveguide region and the central conductor of the resonator. The short constitutes a shunt inductance L_s between the central conductor and the side ground conductors. Both configurations result in half-wavelength resonator over which the standing wave has the current and voltage distributions as those shown in Fig. 5 (a) and 5 (b). A third configuration of transmission line resonators is to terminate a CPW region by a series gap at one of its ends and to terminate the other end by a shunt short as shown in Fig. 5 (c). This creates a quarter-wavelength resonator in which a standing wave exists with the voltage and current distributions presented in the same figure. The CPW region between the two shorts, the two gaps, or the gap and short has a length l_R and constitutes a CPWR which is end-coupled to the main feeder through the terminating gaps or shorts. The gap terminations create capacitive coupling between the CPW feeder and the CPWR, whereas the short terminations create inductive coupling.

For half-wavelength transmission line resonators, the resonant frequencies can be expressed as follows [12]:

$$f_n^{(1/2)} = ,n\,c\ /2l_R\sqrt{\varepsilon_{r_{eff}}}\ n = 1,2,\ldots \qquad \text{(1-a)}$$

where c is the velocity of light in free space, n is the mode order, and $\varepsilon_{r_{eff}}$ is the effective dielectric constant of the quasi-TEM mode of the CPW. For the quarter-wavelength transmission line resonators, the resonant frequencies can be expressed as follows:

$$f_n^{(1/4)} = (2n-1)\,c/l_R\sqrt{\varepsilon_{r_{eff}}},\ n = 1,2,\ldots \qquad \text{(1-b)}$$

The effective dielectric constant of the quasi-TEM mode of the CPW can be expressed as follows [13]:

$$\varepsilon_{r_{eff}} = 1 + \varepsilon_r - 1/2\ K(\acute{k}_0)/K(k_0)\ K(k_1)/K(\acute{k}_1), \qquad (2)$$

where ε_r is the dielectric constant of the substrate material and K denotes the complete elliptic integral of the first kind, which is defined as follows:

$$K(k) = \int_0^{\frac{\pi}{2}} d\theta/\sqrt{1-k\,sin^2\,\theta} \qquad (3)$$

The arguments, k_0, $\acute{k}_0$, k_1, and $\acute{k}_1$, of K are defined as follows:

$$k_0 = s/s+2w,\ \ \acute{k}_0 = \sqrt{1-k_0^2},\ \ k_1 = \sinh(\pi s/4h)/\sinh[\pi(s+2w)/4h],\ \ \acute{k}_1 = \sqrt{1-k_1^2}, \qquad (4)$$

where s is the width of the central conductor, w is the width of each slot, and h is the height of the dielectric substrate. The characteristic impedance of the quasi-TEM mode of the CPW is expressed as follows [13]:

$$Z_0 = 30\pi/\sqrt{\varepsilon_{r_{eff}}}\ K(\acute{k}_0)/K(k_0). \qquad (5)$$

A. Estimation of the quality factor of the bandpass filter

Two types of U-shaped CPWR which are parallel edge-coupled to the L-shaped CPW feeder are shown in Fig. 3. Definitely, the edge coupling between the resonator and the feeding CPW regions has the capacitive coupling effect as regards the external loading

on the resonator. As a consequence, the resonance frequency can be shifted due to the reactive coupling as part of the energy is stored in the electric field of the coupling capacitance. Besides, due to such capacitive coupling, the resultant (loaded) quality factor (Q_l) is decreased as the edge coupling to the feeding transmission lines can be considered as a loss channel. The coupling (external) quality factor Q_e, which is related to the edge (capacitive) coupling between the resonator and the feeder, dominates the resultant (loaded) quality factor. Thus, the total quality factor can be evaluated through the following relation:

$$1/Q_l = 1/Q_u + 1/Q_e, \quad (6)$$

where, Q_u is the self or internal (unloaded) quality factor of the CPWR without being coupled to the feeding transmission line.

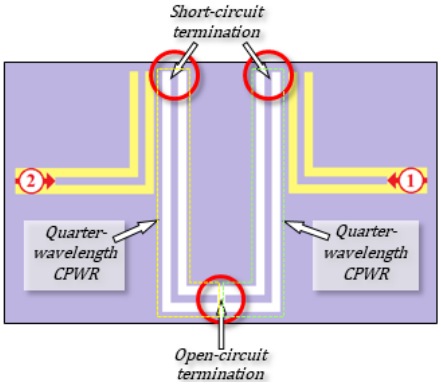

Fig. 3. Dual-bandpass filter based on two mirrored-L-shaped quarter-wavelength resonators subtending and overlapping with a third straight quarter-wavelength resonator.

B. Unloaded quality factor of the half-wavelength CPWR on the perimeter of the U-shape

For the bandpass filter design shown in Fig. 2, the CPW region forming the perimeter of the U-Shape can be considered a short-circuited half-wavelength transmission line resonator. As shown in [14], the unloaded quality factor of both short-circuited and open-circuited half-wavelength CPWR, the quality factor can be expressed as follows:

$$Q_u = \pi/2\alpha l_{R\frac{1}{2}} = \beta_0\sqrt{\varepsilon_{r_{eff}}}/2\alpha = \omega_0\sqrt{\varepsilon_{r_{eff}}}/2c\alpha, \quad (7)$$

where, $l_{R_{1/2}}$ is the length of the half-wavelength resonator, β_0 is the free space wave number, ω_0 is the resonant angular frequency, α is the attenuation constant of the CPW, and $\varepsilon_{r_{eff}}$ is given by (2).

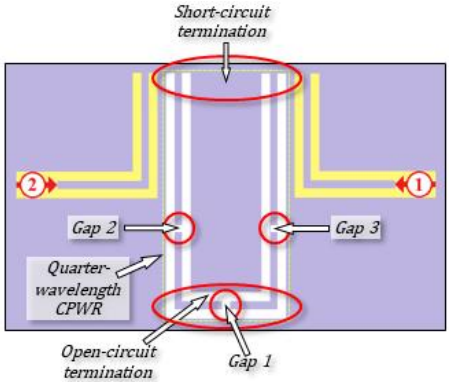

Fig. 4. Single-bandpass filter based on a single quarter-wavelength resonator.

C. Unloaded quality factor of the quarter-wavelength CPWR subtended between the arms of the U-shape

As mentioned in Section II, the CPW region whose center conductor is subtended between the arms of the U-Shape shown in Fig. 2 is open-circuited at one end and short-circuited at the other end and, hence, it can be considered as quarter-wavelength resonator. As shown in [14], a short-circuited quarter-wavelength transmission line has the same expression as (7) for the unloaded quality factor. For open-circuited quarter-wavelength transmission line, the input impedance can be calculated as follows:

$$Z_{in} = Z_0 \tanh \alpha l - j \cot \beta l / 1 - j \tanh \alpha l \cot \beta l. \quad (8)$$

Let $\omega = \omega_0 + \Delta\omega$, and assume $l = l_{R_{1/4}} = \lambda/4$ at ω_0, hence, near the resonance for a TEM line:

$$\beta l \approx \beta l_{R_{1/4}} = \pi/2 + \pi/2\,\Delta\omega/\omega_0. \quad (9)$$

Thus,

$$\cot \beta l_{R_{1/4}} = -\tan \pi/2\,\Delta\omega/\omega_0\,. \quad (10)$$

For low-loss quarter-wavelength transmission line resonator near resonance, $\alpha l_{R_{1/4}} \ll 1$, and $\Delta\omega/\omega_0 \ll 1$, hence,

$$\cot \beta l_{R_{1/4}} \approx -\pi/2\,\Delta\omega/\omega_0\,,\ \tanh \alpha l_{R\frac{1}{4}} \approx \alpha l_{R\frac{1}{4}}. \quad (11)$$

Substituting from (11) into (8), the expression of Z_{in} is reduced to:

$$Z_{in}Z_0\ \alpha l + J\,\pi/2\,\Delta\omega/\omega_0/1 + J\alpha l\,\pi/2\,\Delta\omega/\omega_0. \quad (12)$$

For low loss CPWR in a narrow frequency band around the resonance, one has $\alpha l\Delta\omega/\omega_0 \ll 1$ and, hence the expression (12) can be reduced to take the following form:

$$Z_{in} \approx Z_0(\alpha l + J\,\pi/2\,\Delta\omega/\omega_0). \quad (13)$$

For a resonant series RLC circuit, $\omega_0 = 1/\sqrt{LC}$ and, in a narrow frequency band around the resonance, the circuit impedance can be expressed as follows [14]:

$$Z = R + j2L\,\Delta\omega. \quad (14)$$

By comparison between (13) and (14) one finds,

$$R = Z_0\alpha l, \quad L = Z_0\pi/4\omega_0\,, \quad C = 1/\omega_0^2 L = 4/\pi Z_0\omega_0. \quad (15)$$

Also, for series RLC resonant circuit, the quality factor can be expressed as follows [14]:

$$Q_{RLC} = \omega_0 L/R = 1/\omega_0 RC. \quad (16)$$

Making use of (15) and (16), the unloaded quality factor of an open-circuited quarter-wavelength CPWR can be expressed as follows:

$$Q_u = \pi/4\alpha l_{R_{1/4}} = \beta/2\alpha = \beta_0\sqrt{\varepsilon_{r_{eff}}}/2\alpha = \omega_0\sqrt{\varepsilon_{r_{eff}}}/2c\alpha, \quad (17)$$

where, β_0 is the wavenumber of free space. In general, for low loss transmission line:

$$Z_0 \approx \sqrt{L_T/C_T}\,, \quad \alpha \approx 1/2\,(R_T/Z_0 + G_T Z_0), \quad \beta \approx \sqrt{L_T C_T}\,, \quad (18)$$

where, R_T, L_T, C_T, and G_T are, respectively, the resistance, inductance, capacitance and conductance per unit length of the lumped-element circuit model of the transmission line.

IV. RESULTS AND DISCUSSIONS

In the present section, both the numerical results obtained by simulation and the experimental results obtained by microwave measurements of the fabricated bandpass filter prototypes are presented, discussed and compared for the purpose of arriving at accurate performance assessment and understanding of the resonance mechanisms underlying the filter operation.

It should be noted that the following presentations and discussions of numerical and experimental results are concerned with a dual bandpass filter as that shown in Fig. 2 designed with the following dimensional parameters, unless otherwise stated: $s = s_f = 0.1$ mm, $w = w_f = 0.2$ mm, $W_b = 2.4$ mm, $L_a = 26$ mm, $L_f = 10.3$ mm, $D = 0.35$ mm, and $L = 10.4$ mm. The substrate material has dielectric constant $\varepsilon_r = 3.38$, and height $h = 0.2$ mm. The metal strips and ground are made of copper and have conductivity $\sigma = 5.6 \times 10^7$ S/m. It should be noted that other materials are assumed when presenting the results concerned with filters designs based on superconducting CPWR which is indicated during the discussions.

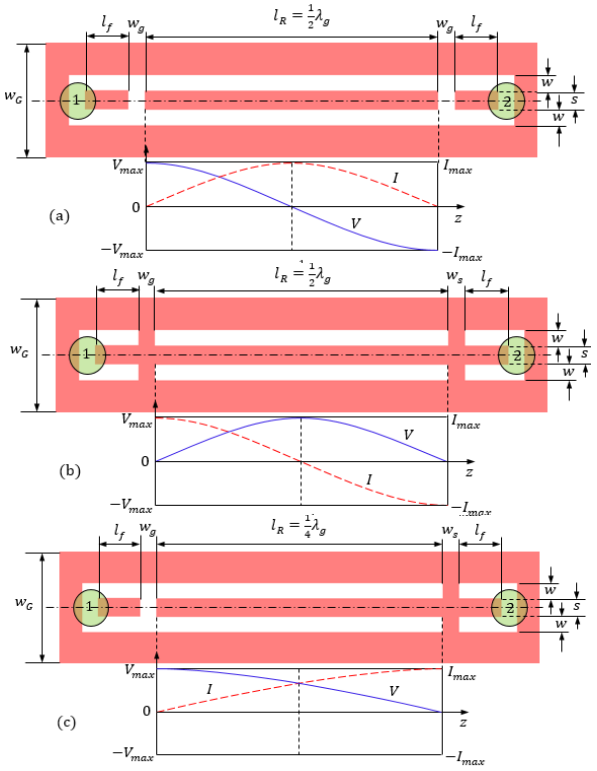

Fig. 5. Different regimes of CPW resonators: (a) open-ended, half-wavelength CPWR, (b) short-ended half-wavelength CPWR, and (c) open/short-ended quarter-wavelength CPWR.

A. Performance comparison of multi-resonator BPF

This section is dedicated for the performance comparison of cascaded dual-band BPF employing single, double, and triple resonators arranged as shown in Fig. 1 (a). The design dimensions are $w = 0.4$ mm, $L_a = 15.3$ mm, $L = 14$ mm, $L_f = 4.4$ mm, $s_f = 0.5$ mm, $w_f = 0.4$ mm, $W_b = 1$mm, $D = 0.2$ mm, $Dr = 0.1$mm. The frequency response of the transmission coefficient of the first band centered at 2.02 GHz for the BPF composed of one, two, and three resonators is plotted in Fig. 6. It is clear in the figure that the design of the BPF constructed from single dual-band resonator has a sharp behavior and narrower bandwidth than the designs employing double and triple resonators. The quality factor is also higher for a BPF with single resonator. For this reason, the next discussions will deal with the results of performance assessment of BPF composed of only single resonator.

B. Frequency response of bandpass filter based on half-wavelength CPWR of U-shape

The frequency response of the transmission

coefficients $|S_{21}|$ of the proposed dual bandpass filter having the same design as that shown in Fig. 2, under the assumption of perfect conductor and lossless dielectric substrate, is presented in Fig. 7. The frequency response exhibits two sharp peaks: the first peak is at $f = 1.9405$ GHz , with quality factor $Q = 6130$, whereas the second peak is at $f = 2.169$ GHz, with quality factor $Q = 1000$. The mechanisms of resonance leading to these values of the resonant frequencies and the corresponding quality factors are explained in the following subsection.

The two corner-shaped CPW regions of the main feeder are coupled to each other only at the resonances of each of the two CPW resonators formed by the U-shape as mentioned above. The frequency response of the filter transfer function has two sharp peaks as shown in Fig. 7. The first peak corresponds to the first resonance of the half-wavelength CPW resonator on the perimeter of the U-shape which is short-circuited terminated at its both ends. The second peak corresponds to the first resonance of the quarter-wavelength CPW resonator whose central conductor is the area subtended between the arms of the U-shape. The side (ground) conductors for this CPW are actually the central conductor of the CPW on the perimeter of the U-shape mentioned above. As shown in the sketch of the geometry presented in Fig. 2, these side conductors have much narrower width in comparison to the width of the central conductor. This resonator is open circuit terminated at the base of the U-shape and is short-circuit terminated at the other end. This is more elaborated showing illustrations of the current and field distributions on the resonator in the following two subsections.

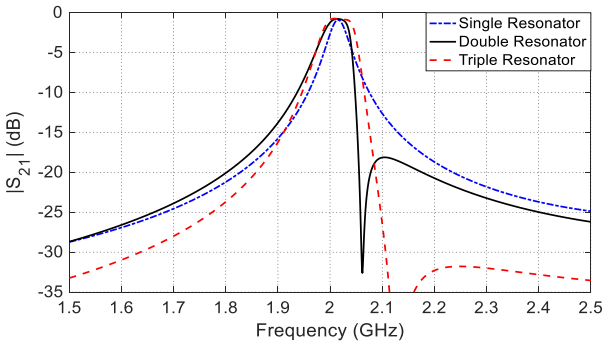

Fig. 6. $|S_{21}|$ for the first band of cascaded dual-band BPF designed with one, two, and three resonators.

B.1. Mechanism of resonance in the lower pass Band

At the lower resonant frequency (1.9405 GHz) of the short-circuit-terminated CPWR formed by the perimeter of the U-shape, the surface current distribution is presented in Fig. 8. It is shown that, like a short-ended half-wavelength resonator, as explained in Section III and illustrated in Fig. 5 (b), the current has its maximum magnitude at the short-circuited terminals of the resonator whereas the current node of the standing wave is at the middle of the resonator length. The electric field distribution in the slots of this CPW is presented in Fig. 8 which exhibits the behaviour of the (even) quasi-TEM mode of the CPW formed by the arms of the U-shape. As this CPW region is a half-wavelength resonator whose total length is 55.2 mm, the resonant frequency can be calculated using (1-a), which gives $f_0^{(1/2)} = 1.914$ GHz. The slight deviation of the resonant frequency obtained by simulation from the theoretical value given by (1-a) can be attributed to the reactive load resulting from coupling the CPW feeder to the CPWR as part of the energy is stored in the electric field of the coupling capacitance and, thereby causing a shift of the resonant frequency . Moreover, a part of the frequency shift can be attributed to the error of the approximate analytic formula for $\varepsilon_{r_{eff}}$ given by (2).

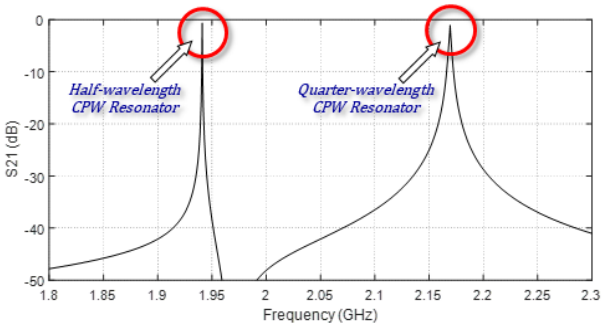

Fig. 7. Frequency response of the bandpass filter (with the design shown in Fig. 2) based on half-wave length CPWR with U shape subtending another quarter-wavelength CPWR.

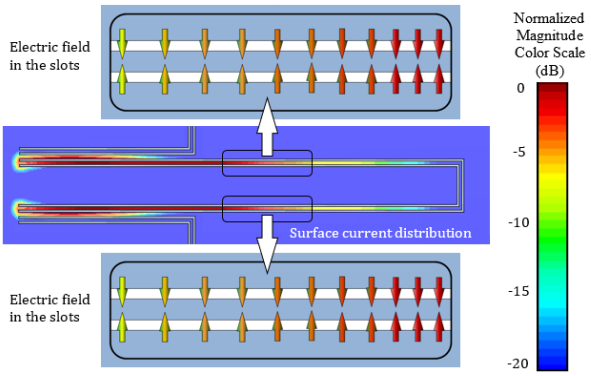

Fig. 8. Surface current on the conductors and electric field distribution in the slots at the resonant frequency corresponding to the short-circuit terminated half-wavelength CPW resonator, $f = 1.9405$ GHz.

B.2. Mechanism of resonance in the upper pass band

At the higher resonant frequency (2.169 GHz) of the CPWR whose central conductor is the region subtended between the arms of the U-shape, the surface current distribution is presented in Fig. 9. This CPW region is open-circuit terminated at the base of the U-shape and is short-circuit terminated at its other end. It is shown that, like a quarter-wavelength resonator, as explained in Section II and illustrated in Fig. 5 (c), the current has its maximum magnitude at the short-circuit terminal whereas the current node is at its open-circuit terminal. As this CPW region is a quarter-wavelength resonator whose length is 26.0 mm, the resonant frequency can be calculated using (1-b), which gives $f_0^{(1/4)} = 2.311$ GHz. In addition to the approximation error of the analytical formula given by (2) for $\varepsilon_{r_{eff}}$, the slight deviation of the resonant frequency obtained by simulation from the theoretical value given by (1-b) can be attributed to the reactive load resulting from coupling the CPW feeder to the CPWR as part of the energy is stored in the electric field of the coupling capacitance and, thereby causing a shift of the resonant frequency.

C. Frequency response of BPF based on quarter-wavelength CPWR with mirrored-L shape

For the bandpass filter design shown in Fig. 3, which is based on two identical quarter-wavelength CPWRs forming a Mirrored-L shape, the corresponding frequency response of the transmission coefficient, $|S_{21}|$, of a lossless filter is shown in Fig. 10. By comparison to the bandpass filter of the design shown in Fig. 2, whose frequency response is presented in Fig. 7, it is shown that their frequency responses of the transmission coefficients seem to be identical. However, this is not actually true as the quality factor at the lower frequency band for the filter design based on two quarter-wavelength resonators concerned in this section is $Q = 14{,}300$, which is much higher than that obtained by the filter design shown in Fig. 2 whose quality factor is $Q = 6{,}130$ as presented in Section IV.A. Also, the quality factor for the upper pass band is improved from $Q = 1{,}000$ for the old design to $Q = 1{,}100$ for the new design. The results for comparison between the two designs are presented in Table 1. Thus, the main advantage of the gap made in the central conductor at the middle of the base of the U-shape is the considerable improvement of the quality factor especially for the lower pass band.

D. Effect of dielectric losses on the performance of the bandpass filter based on CPWR

It is well-known that the quality factor of a resonant structure is reduced with increasing the losses. The purpose of the present section is the quantitative assessment of dependence of the quality factor of the proposed bandpass filter on the dielectric losses of the substrate material.

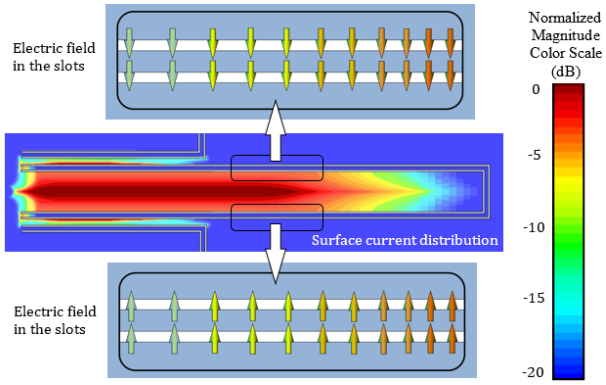

Fig. 9. Surface current on the conductors and electric field distribution in the slots of the CPWR at the resonant frequency corresponding the quarter-wavelength CPWR subtended between the arms of the U-shape, $f = 2.169$ GHz.

Table 1: Comparison between the resonant frequencies and quality factors of the bandpass filter designs shown in Fig. 2 and Fig. 3

Base of U-shape	Lower Pass Band			Upper Pass Band		
	Resonance Regime	f_0 (GHz)	Q	Resonance Regime	f_0 (GHz)	Q
Solid	1/2-Wavelength	1.9405	6130	1/4-Wavelength	1.1695	1000
Slotted	1/4-Wavelength	1.9404	14300	1/4-Wavelength	1.1697	1100

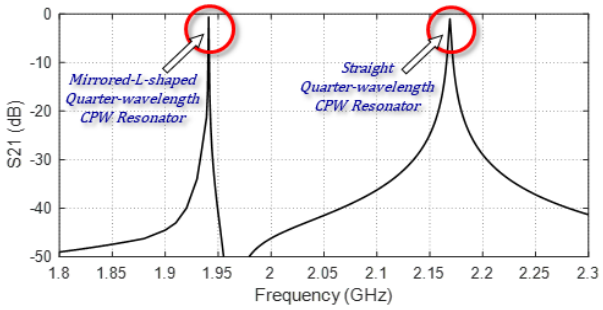

Fig. 10. Frequency response of the bandpass filter (with the design shown in Fig. 3 based on two identical quarter-wavelength CPWRs forming a mirrored-L shape.

D.1. Effect of dielectric loss on the quality factor of the half-wavelength CPWR with U-shape

The effects of the losses of the dielectric substrate on the filter response at the lower and higher frequency pass bands are presented in Fig. 11. It is shown that, for the lower and upper bands, the peak of $|S_{21}|$ is decreased, the bandwidth is increased and, consequently, the quality factor is significantly decreased with increasing the loss tangent ($\tan\delta \approx \delta$) of the substrate material. Generally,

the bandpass performance is considerably degraded with increasing the dielectric losses. Due to its higher quality factor, the lower frequency pass band is considerably more affected by the dielectric loss than the higher frequency pass band.

D.2. Effect of dielectric loss on the quality factor of the quarter-wavelength CPWR with mirrored-L shape

The higher the quality-factor of a resonator, the worse the effect of losses on the frequency response of its transfer function. As discussed in Section IV-C, the bandpass filter employing a quarter-wavelength CPWR with mirrored-L shape has a considerably higher quality factor than that of the bandpass filter employing half-wavelength U-shaped CPWR. As a consequence, the quality factor of the former bandpass filter is more badly affected by the dielectric losses. This may be more clear when investigating the frequency response of the of the transmission coefficients $|S_{21}|$ for this filter which is presented in Fig. 12.

D.3. Comparison between the effects of dielectric loss on the quality factors of single half-wavelength and double quarter-wavelength resonators

The dependence of the quality factor on the dielectric loss tangent of the substrate material for the bandpass filter employing U-shaped half-wavelength CPWR subtending another quarter-wavelength CPWR, in comparison to that employing two quarter-wavelength CPWRs of mirrored-L shape subtending a third quarter wavelength CPWR, is presented in Fig. 13. In the lower pass band the quality factor obtained in the case of double quarter-wavelength resonator is much larger than that obtained by employing single half-wavelength resonator over the indicated range of δ as shown in Fig. 13 (a). By comparing the Q-δ relation in the lower pass band, presented in Fig. 13 (a) to the Q-δ relation in the upper pass band, presented in Fig. 13 (b), it becomes clear that the quality factor rapidly decays with increasing the loss tangent in a manner such that the higher the quality-factor the higher the slope of decay. Also, by comparing the slopes of the Q-δ curves for the two pass bands it becomes clear that the decay of Q with increasing δ for the lower pass band is considerably steeper than that of the upper pass band due to the considerable larger value of Q in the lower pass band for both filter designs.

E. Experimental assessment of dual-bandpass filters based on Dual-CPWR

The purpose of the experimental work is to study the underlying physical principles of operation and to investigate the performance of the proposed high quality factor bandpass filter based on dual-resonance mechanism.

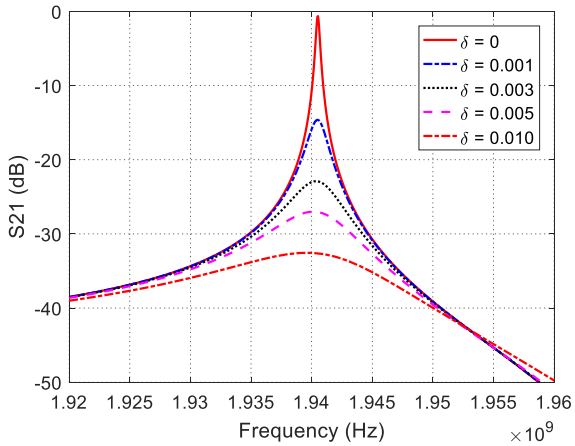

(a) Filter response in the lower pass band

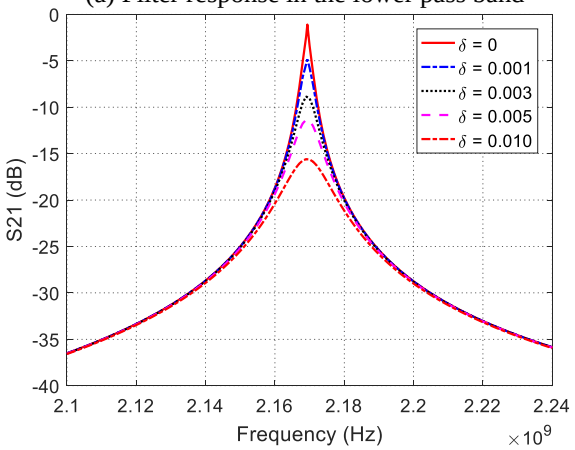

(b) Fiter response in the higher pass band

Fig. 11. Effect of dielectric substarte loss on the frequency response of the transmission coefficients $|S_{21}|$ for the BPF based on half-waevlength CPWR with U-shape.

E.1. Fabrication of prototypes for the proposed bandpass filter

Three prototypes of the proposed bandpass filter are fabricated for experimental studying of the underlying physical principles of operation. The substrate used for fabrication is RO4003C™, with substrate height $h = 0.2$ mm, dielectric constant $\varepsilon_r = 3.38$ and dielectric loss tangent $\delta = 0.0021$ at 2.5 GHz. The same design dimensions given at the beginning of section IV are used for fabrication. A photograph of the fabricated prototypes is presented in Fig. 14.

Prototype '1' is fabricated for the bandpass filter design shown in Fig. 2 with the dimensional parameters given at the beginning of Section IV. This filter is composed of a U-shaped half-wavelength CPWR overlapping with another quarter-wavelength CPWR of wide central conductor which is sandwiched between the arms of the U-shape.

The prototype '2' is fabricated for the bandpass filter design shown in Fig. 3. Its shape similar to that of prototype '1' with a basic difference is that the single half-wavelength U-shaped CPWR is replaced by two identical quarter-wavelength resonators forming a shape of mirrored-L as shown in Fig. 3. This is simply achieved by modifying prototype '1' by cutting a gap in the central conductor at the middle point of the base of the U-shaped CPWR. Thus, the resulting prototype '2' can be considered as bandpass filter composed of three quarter-wavelength CPW resonators which are parallel and overlapped.

Prototype '3' is fabricated for the bandpass filter design shown in Fig. 4. It is made by modifying prototype '2' by etching two other gaps each gap is cut in one of the two quarter-wavelength resonators forming the mirrored-L of prototype '2'. The purpose of these gaps is to damp or reduce the resonance of the two quarter-wavelength CPW resonators forming the mirrored-L so as to get prototype '3' working as a high-quality-factor single-bandpass filter.

E.2. Experimental setup

The vector network analyzed (VNA) of the Keysight (Agilent) FieldFox N9928A is used to measure the transmission and reflection coefficients $|S_{21}|$ and $|S_{11}|$, respectively, of the bandpass filter prototype under test. For this purpose the filter prototype is mounted on the substrate test fixture as shown in Fig. 15 (a). After performing the required settings and calibration procedure, the test fixture holding the prototype under test is connected to the VNA as shown in Fig. 15 (b).

E.3. Experimental results

It should be noted that, for the three fabricated prototypes shown in Fig. 14, the bandpass filters have the designs shown in Figs. 2, 3, and 4, respectively, with the values of the design parameters given at the beginning of Section IV, in addition to the following dimensions for the gaps cut in the central conductors as modifications of the original filter design: $g_v = g_h = 0.2$ mm, $d_v = 1.25$ mm, and $d_h = 5.1$ mm.

The frequency response of the transmission coefficient of the prototype '1' for the proposed bandpass filter as measured by the VNA is presented in Fig. 16 and compared to that obtained by simulation using the commercially available CST® software package. Both the experimental and simulation results show that the peak of $|S_{21}|$ in the lower pass band is considerably more decreased due to the dielectric losses than that of the upper pass band. The experimental measurements and simulation results show good agreement except for a little shift of the resonant frequency of the lower band, which is, most probably, attributed to the losses encountered in the measurement process.

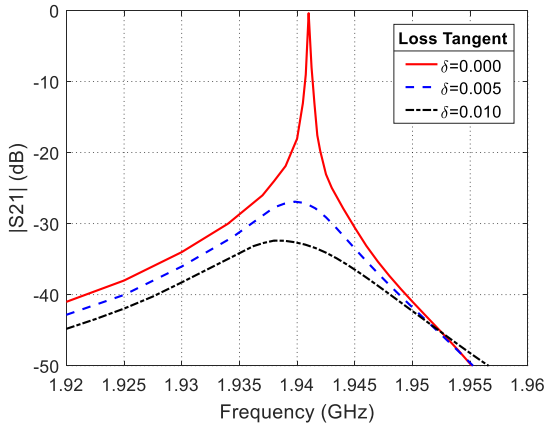

(a) Filter response in the lower pass band

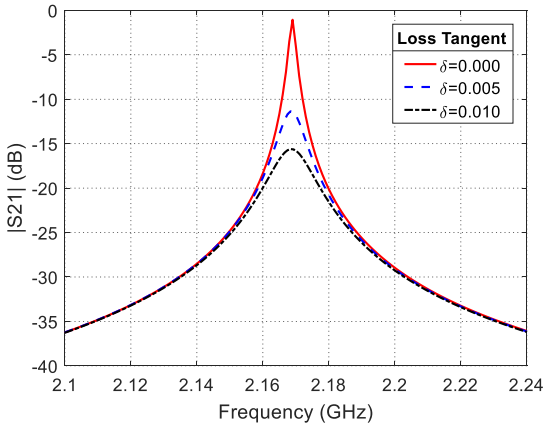

(b) Filter response in the higher pass band

Fig. 12. Effect of dielectric substarte loss on the frequency response of the transmission coefficients $|S_{21}|$ for the bandpass filter based on quarter-wavelength CPWR with mirrored L-shape.

The frequency response of the transmission coefficient of prototype '2' which is fabricated for a bandpass filter employing double quarter-wavelength CPWR subtending a third quarter-wavelength CPWR as measured by the VNA is presented in Fig. 17 and compared to that obtained by simulation using the CST® software package. Both the experimental and simulation results show that the peak of $|S_{21}|$ in the lower pass band is considerably more decreased due to the dielectric losses than that obtained for the bandpass filter prototype '1' due to the considerably higher quality factor of the former bandpass filter. This comes in agreement with the simulation results presented in both Figs. 11 and 12 where the quality factor of the lower frequency pass band is shown to be more degraded due to the dielectric loss than that of the upper pass band. Thus, both the simulation and experimental results leads us to arrive at the same conclusion: the higher the quality factor the worse the effect of the dielectric loss on the bandpass

filter response. Also, the experimental measurements and simulation results show good agreement except for a little shift of the resonant frequency of the lower band, which is, most probably, attributed to the losses encountered in the measurement process.

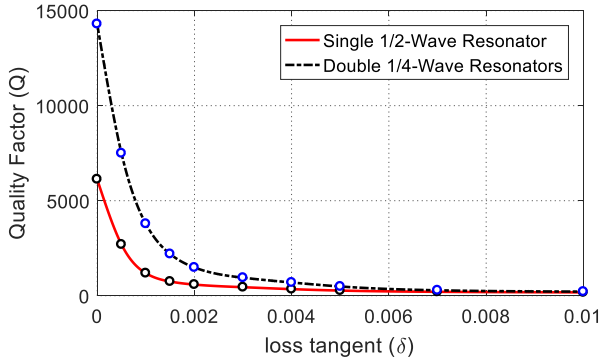

(a) Q versus δ for the lower pass band

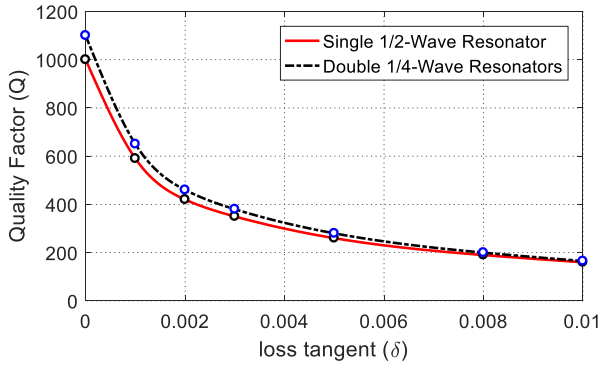

(b) Q versus δ for the higher pass band

Fig. 13. Comparing the dependence of the quality factor, Q, on the dielectric loss tangent, δ, for the bandpass filter with half-wavelength CPWR of U shape to that of the bandpass filter with two quarter-wavelength CPWRs forming a mirrored-L shape.

The prototype '3' is fabricated for a single-bandpass filter that employs a single quarter-wavelength CPWR and, hence, exhibits a single resonance. The frequency responses of the transmission and reflection coefficients $|S_{21}|$ and $|S_{11}|$, respectively, of this filter are presented in Fig. 18. The measurements are achieved by the VNA and compared to that obtained by simulation using the CST® software package. The experimental measurements and simulation results show good agreement. The quality factor obtained for the fabricated prototype '3' of the proposed single-bandpass filter is $Q = 102$, whereas that calculated through simulation is $Q = 167$. The deviation of the measured quality factor than that calculated by simulation is most probably attributed to the losses encountered in the measurement process.

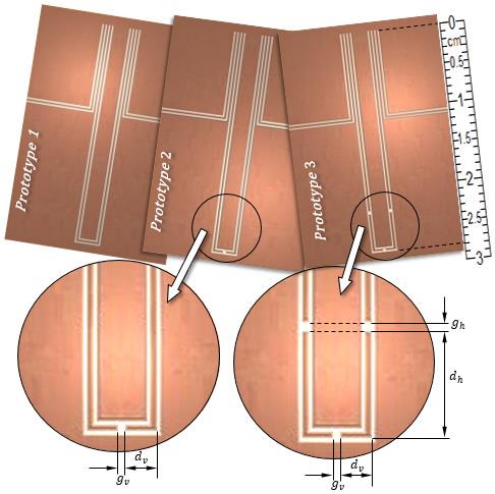

Fig. 14. Three fabricated prototypes for the proposed high quality bandpass filter.

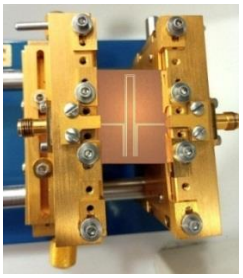

(a) The fabricated BPF mounted on the VNA test fixture

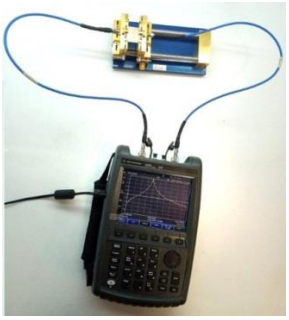

(b) The test fixture connected to the VNA

Fig. 15. Measurement of the frequency response of the fabricated prototypes.

F. Improvement of the quality factor of the bandpass filter

As mentioned in the introduction of the present paper, the high quality-factor superconducting CPWR is required in many applications such as a quantum data bus for hybrid quantum information systems. In this section, some modifications of the proposed BPF design are suggested to increase the quality factor so as to be

valid for applications like that mentioned above when it is fabricated form a metal that exhibits superconductivity at achievable low Kelvin temperature and printed on a substrate of a lossless dielectric material. Thus the dual-resonant structure is constructed as superconductor CPWR printed on a lossless dielectric substrate.

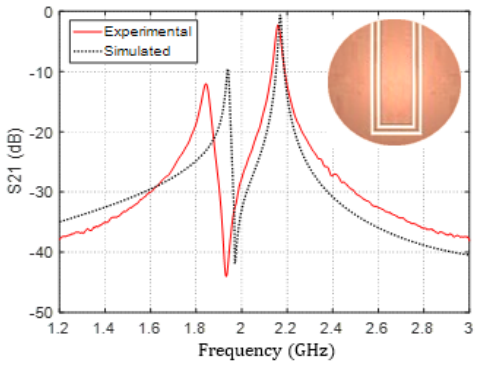

Fig. 16. Frequency response of the transmission coefficient $|S_{21}|$ of the BPF prototype '1' of the original (No-gap) filter design.

F.1. Dual-band BPF based on open-circuited U-shaped CPWR

It may be interesting to investigate the bandpass filter response when the short-circuit terminations at the ends of the CPWR formed by the perimeter of the U-shape, presented in Fig. 2, are replaced by open-circuit terminations. It is expected that such a replacement may lead to a significant change of the filter response at its lower pass band due the major change of the current distribution along the arms of the U-shape at its resonant frequency. As the quarter-wavelength CPWR whose central strip is the area subtended between the arms of the U-shape is geometrically unaffected by the termination replacement, it is expected that the filter response at its upper pass band will not be significantly different from the response of the previous design in this band of the frequency.

F.2. Comparison between short-circuited and open-circuited U-shaped CPWR bandpass filter

A comparison between the frequency responses of the transmission coefficients, $|S_{21}|$, for bandpass filters employing short-ended and open-ended half-wavelength CPW resonator of U shape is presented in Fig. 19. It is clear that the open-circuit termination of the U-shaped resonator results in a considerably higher quality factor as listed in Table 2. A quality factor of 3.71×10^4 is obtained by the open-ended superconducting CPWR printed on a lossless dielectric substrate in the lower pass band (about 6 times that obtained with the short-ended CPWR). On the other hand, by comparing the frequency responses of the filters with open-ended and short-ended U-shaped resonators in the upper pass band, Fig. 19 (b), it seems that the design modification results in a slight shift of the resonant frequency associated with a slight reduction of the quality factor as given in Table 2.

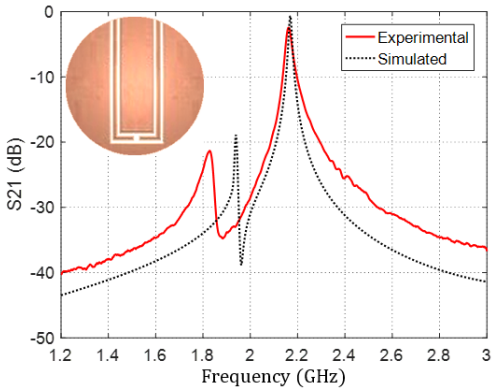

Fig. 17. Frequency response of the transmission coefficient $|S_{21}|$ of the bandpass filter prototype '2' of the 'one-gap' design.

Table 2: Resonant frequency and quality factor of the bandpass filter for the possible termination types of the U-shaped CPWR

Termination of CPW Resonator	Lower Pass Band		Upper Pass Band	
	f_0(GHz)	Q	f_0(GHz)	Q
Short	1.9405	6.13×10^3	1.1695	1070
Open	1.9450	3.71×10^4	1.1605	905

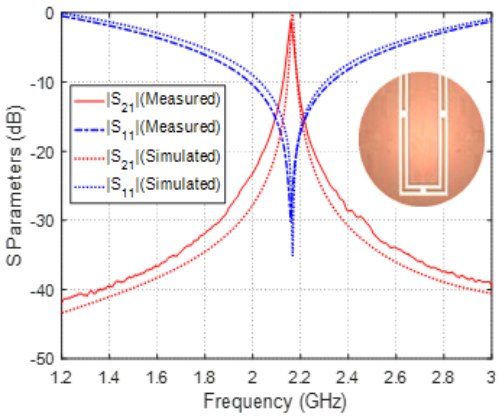

Fig. 18. Frequency response of the transmission and reflection coefficients $|S_{21}|$ and $|S_{11}|$, respectively, of the BPF prototype '3'.

F.3. Mechanism of resonance in the lower frequency band for open-circuit termination

At the lower resonant frequency (1.9451 GHz) of the open-circuit terminated CPWR on the perimeter of the U-shape, the surface current distribution is presented in Fig. 20. It is shown that, like an open-ended half-

wavelength resonator as explained in Section II and illustrated in Fig. 5 (a), the current has its maximum magnitude at the middle of the resonator length whereas the current nodes of the standing wave are at the open-end of the CPWR.

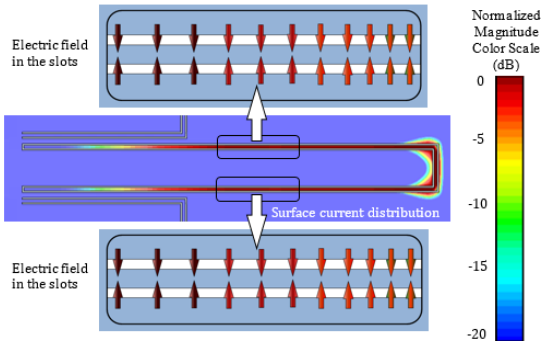

Fig. 19 Surface current on the conductors and electric field distribution in the slots at the resonant frequency corresponding the open-circuit terminated half-wavelength CPW resonator, $f = 1.9451$ GHz.

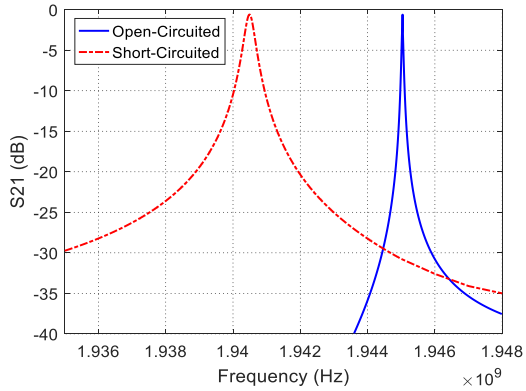

(a) Frequency response in the lower pass band

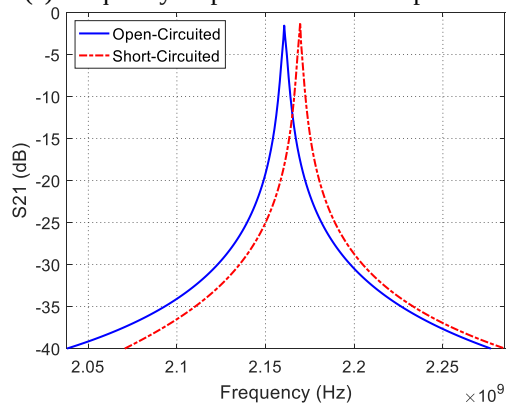

(b) Frequency response in the upper pass band

Fig. 20. Comparison between the frequency response of the transmission coefficients $|S_{21}|$ for the bandpass filters with open-circuit and short-circuit terminated U-shaped half-wavelength CPWRs.

A comparison of the proposed BPF with BPFs found in literature is presented in Table 3.

Table 3: Comparison with similar works

	Size ($\lambda_g \times \lambda_g$)	S_{21}(dB)	S_{11}(dB)
Proposed BPF	0.3×0.21	0.33	-27
[15]	0.25×0.25	1.3	-25
[16]	0.5×0.5	0.1	-25
[17]	0.75×0.6	0.04	-23

VI. CONCLUSION

High quality factor bandpass filter based on a number of cascaded dual-resonance CPW resonators is proposed. Each resonant structure is constructed as two overlapped CPWRs. The cascaded resonators mediate microwave coupling between two isolated CPW feeders only at the resonant frequencies leading to a bandpass filter of high quality factor. Each resonator has its two resonances first-order, where the resonant frequencies and the separation between them can be fine-tuned by the dimensions of the structure. The current distribution on the conducting strips and the electric field distributions in the slots are presented to demonstrate the mechanism of operation of the proposed bandpass filter designs. The effects of the loss tangent of the dielectric substrate material on the quality factors at the two resonant frequencies are presented and discussed. Some experimental results concerned with the frequency response of three fabricated prototypes for three different designs are presented showing good agreement when compared with the corresponding simulation results. It is shown that, at low enough temperature, the proposed structure can operate as superconducting microwave resonator when made from the appropriate materials. An optimized design of the proposed bandpass filter, based on superconducting CPWR structure, is shown to achieve quality factors high enough to form a quantum data bus for hybrid architecture of quantum information systems.

REFERENCES

[1] J. K. A. Everard and K. K. M. Cheng, "High performance direct coupled bandpass filters on coplanar waveguide," *IEEE Transactions on Microwave Theory and Techniques*, vol. 41, no. 9, pp. 1568-1573, 1993.

[2] K. C. Gupta, R. Garg, and I. Bahl, *Microstrip Lines and Slotlines*, Dedham, MA Artech, 1979.

[3] A. Gopinath, "Losses in coplanar waveguides," *IEEE Transactions on Microwave Theory and Techniques*, vol. 30, no. 7, pp. 1101-1104, 1982.

[4] F. D. Williams and S. E. Schwarz, "Design and performance of coplanar waveguide bandpass filters," *IEEE Transactions on Microwave Theory and Techniques*, vol. 31, no. 7, pp. 558-566, 1983.

[5] M. Göppl, A. Fragner, M. Baur, R. Bianchetti, S. Filipp, J. M. Fink, P. J. Leek, G. Puebla, L. Steffen, and A. Wallraff, "Coplanar waveguide resonators for circuit quantum electrodynamics," *Journal of Applied Physics*, vol. 104, no. 11, p. 113904, 2008.

[6] H.-J. Li, Y.-W. Wang, L.-F. Wei, P.-J. Zhou, Q. Wei, C.-H. Cao, Y.-R. Fang, Y. Yu, and P.-H. Wu, "Experimental demonstrations of high-Q superconducting coplanar waveguide resonators," *Chinese Science Bulletin*, vol. 58, no. 20, pp. 2413-2417, 2013.

[7] M. Kumar and R. Gowri, "Review on various issues and design topologies of edge coupled coplanar waveguide filters," *Journal of Graphic Era University*, vol. 5, no. 2, pp. 91-96, 2017.

[8] M. Kumar and R. Gowri, "Analysis and characterization of edge coupled coplanar waveguide discontinuities for filter applications," *Proceedings of the Sixth International Conference on Computer and Communication Technology, ACM*, pp. 309-312, Sep. 2015.

[9] R. El Haffar, A. Farkhsi, O. Mahboub, and N. A. Touhami, "Compact size coplanar waveguide bandpass filter design and modeling," *Proceedings of the 2nd International Conference on Computing and Wireless Communication Systems, ACM*, p. 49, Nov. 2017.

[10] M. Kumar and R. Gowri, "Design of compact and high performance edge coupled coplanar waveguide band pass filter," *IEEE 1st International Conference on Power Electronics, Intelligent Control and Energy Systems (ICPEICES)*, pp. 1-3, July 2016.

[11] T. M. Weller, "Edge-coupled coplanar waveguide bandpass filter design," *IEEE Transactions on Microwave Theory and Techniques*, vol. 48, no. 12, pp. 2453-2458, 2000.

[12] D. Bothner, M. Knufinke, H. Hattermann, R. Wölbing, B. Ferdinand, P. Weiss, R. Kleiner, P. Weiss, S. Bernon, J. Fortagh, D. Koelle, and R. Kleiner, "Inductively coupled superconducting half wavelength resonators as persistent current traps for ultracold atoms," *New Journal of Physics*, vol. 15, no. 9, p. 093024, 2013.

[13] R. N. Simons, *Coplanar Waveguide Circuits, Components, and Systems*, John Wiley & Sons, vol. 165, 2004.

[14] D. M. Pozar, *Microwave Engineering*, John Wiley & Sons, Inc., 2012.

[15] B. George, N. S. Bhuvana, and S. K. Menon, "Compact band pass filter using triangular open loop resonator," *Progress in Electromagnetics Research Symposium*, Nov. 19-22, 2017.

[16] M. S. S. Subramanian, K. V. Siddharth, S. N. Abhinav, V. V. Arthi, K. S. Praveen, R. Jayavarshini, and G. A. S. Sundaram, "Design of dual log-spiral metamaterial resonator for X-band applications," *2012 International Conference on Computing, Communication and Applications (ICCCA)*, 2012.

[17] A. Boutejdar, A. Darwish, and A. Omar, "Design and improvement of compact half-wavelength band pass filter employing overlapped slotted ground structure (SGS) and multilayer technique," *Applied Computational Electromagnetics Society (ACES) Journal*, vol. 28, no. 8, Aug. 2013.